Int. J. Electrochem. Sci., 9 **(2014)** 569 - 579

International Journal of
ELECTROCHEMICAL
SCIENCE
www.electrochemsci.org

Homogeneous Electro-Fenton Oxidative Degradation of Reactive Brilliant Blue Using a Graphene Doped Gas-Diffusion Cathode

Xiaochen Xu, Jie Chen, Guoquan Zhang, Yan Song, Fenglin Yang*

Key Laboratory of Industrial Ecology and Environmental Engineering (MOE), School of Environmental Science and Technology, Dalian University of Technology, Dalian 116024, P.R. China
*E-mail: zhgqdut@gmail.com

Received: 28 September 2013 / *Accepted:* 19 November 2013 / *Published:* 8 December 2013

A novel graphene doped gas diffusion electrode (GE/graphite-PTFE GDE) was prepared in this work with graphite powder and PTFE as starting materials. An undivided electro-Fenton system with this self-made GDE as cathode was fabricated to evaluate the activity of GE/graphite-PTFE GDE for H_2O_2 electro-generation. Compared with bare graphite-PTFE GDE, the electro-generated H_2O_2 concentration on GE/graphite-PTFE GDE was improved three times and can be reached to ca. 187 mg/L after 3 h electrolysis. The maximum production of H_2O_2 was obtained at pH 3.0, the current density of 2.0 mA/cm^2 and $M_{graphite}$:M_{GE}:M_{PTFE} = 8:1:2. The influences of operating parameters including solution pH and Fe^{2+} concentration were investigated on Reactive brilliant blue (KN-R) removal by the proposed electro-Fenton oxidation process. Under the optimal condition, nearly 80% of KN-R and 33.3% total organic carbon (TOC) could be removed after 180 min electrolysis, indicating that the GE/graphite/PTFE GDE was effective in H_2O_2 electro-generation and the proposed homogeneous electro-Fenton system was effective in KN-R oxidative degradation.

Keywords: Graphene; Gas diffusion cathode; Electro-Fenton; H_2O_2; Reactive Brilliant Blue

1. INTRODUCTION

Wastewater generated by textile industriescontains considerable amounts of dyes. It is well known that some dyes and degradation products such as aromatic amines are highly carcinogenic [1]. It is a challenge to remove dyes from wastewater because the traditional treatment processes has been proved to be insufficient [2-4]. Recently, electro-Fenton methods, which combine with ferrous ion (Fe^{2+}) addition and the in-situ electrogenerated H_2O_2 have attracted much attention, since they have been widely used to treat various dyes wastewater [5-8]. Advantages of electro-Fenton are numerous,

including ease of control, amenability to automation, high efficiency, and environmental compatibility, etc [9]. In electro-Fenton process, H_2O_2 can be produced by a two-electron reduction of oxygen (equation (1)) at appropriate cathodic potential on certain electrodes such as reticulated vitreous carbon, graphite and gas diffusion electrode (GDE) [5,6,10,11].

$$O_2 + 2H^+ + 2e^- \rightarrow H_2O_2 \qquad (1)$$

Hydroxyl radicals (•OH) are generated in the solution by the well-known Fenton's reaction between Fe^{2+} and electrogenerated H_2O_2 (equation (2)).

$$Fe^{2+} + H_2O_2 \rightarrow Fe^{3+} + OH^- + HO^{\bullet} \qquad (2)$$

Cathode materials, which have high H_2O_2 production ability, are very important for the oxidation ability of electro-Fenton system. Recently, cathode materials, such as carbon/polytetrafluoroethylene (C/PTFE) GDE [5,6,10,11], graphite [12-14], carbon nanotubes [15], carbon felt [16-19], and reticulated vitreous carbon [20,21] are used as electrode materials for the electrochemical production of H_2O_2. Graphene (GE) has emerged as an interesting material because of its particular nanostructure, outstanding electron-transfer capacity, good stability and large accessible surface area [22,23]. Considering its remarkable properties and its relatively easy preparation approach, the novel GDE was prepared with GE, graphite powder and PTFE in this work. The electroactive surface area of this self-made GDE was characterized by the electrochemical methods. The activity, current efficience and the stability of this self-made GDE for the electrogeneration of H_2O_2 was investigated in detail. Reactive brilliant blue (KN-R) was used as a model anthraquinone dye and was degraded by the electro-Fenton process in an undivided cell. The influence of various parameters on KN-R removal such as pH and concentration of Fe^{2+} were systematically evaluated.

2. EXPERIMENTAL

2.1. Reagent and material

Table 1. Physicochemical properties of Reactive Brilliant Blue (KN-R)

Chemical name	Reactive Brilliant Blue (KN-R)
Chemical formula	$C_{22}H_{16}N_2Na_2O_{11}S_3$
Chemical structural	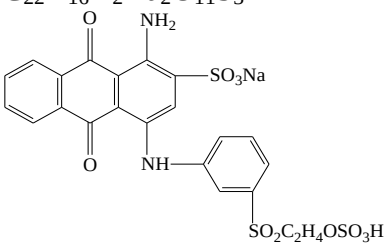
Molecular Weight	626.56
Class	Anthraquinone
Maximum absorption wavelength	590 nm

Graphite powder (600 mesh, analytical grade), PTFE (60%) and stainless steel mesh (20 mesh) were purchased from Beijing Chemical Regent Plant (China). $NaNO_3$, $KMnO_4$ and H_2O_2 (30 wt%)

were of analytical grade and obtained from Shanghai Chemical Reagent Co. (China). Reactive Brilliant Blue (KN-R, analytical grade) was purchased from Tianjing Kemi-ou Chemical Regent Co. (China) and its physicochemical properties are shown in Table 1.

Allother chemicals including H_2SO_4, anhydrous Na_2SO_4, NaOH, $FeSO_4 \cdot 7H_2O$, $TiOSO_4 \cdot 2H_2O$ and anhydrous ethanol were of analytical grade. Deionized water was used in all the experiments.

2.2. Fabrication of GDE

Graphene (GE) was obtained by chemical oxidated graphene oxide, which was synthesized from natural graphite powder using a modified Hummers' method [24,25]. Graphite powder, GE and PTFE solution with the mass ratio of 100:1:2, 50:1:2 and 8:1:2 were added and mixed respectively in an ultrasonic bath for 15 min at room temperature. The mixture was stirred at about 80°C until it became ointment, and then was put into the cylinder mold and formed a circle sheet (4 cm diameter, 1.5 mm thickness) by pressed at 15 MPa for 2 min. The fabricated GE/graphite-PTFE GDEs were finally obtained by calcinations at 300 ˚C for 2 h (Fig. 1).

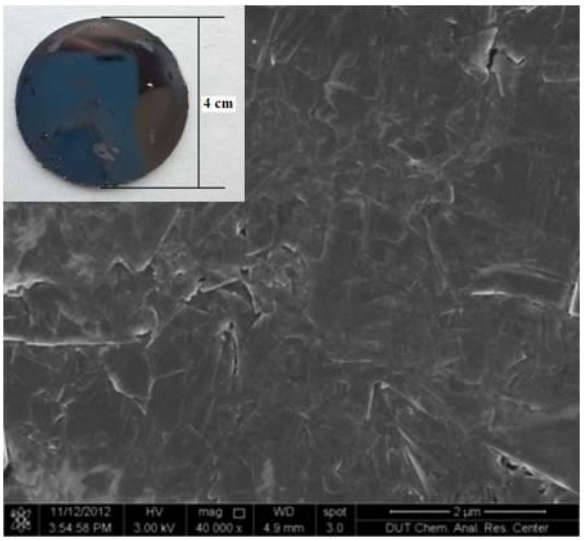

Figure 1. Photograph (inset) and SEM image of GE/graphite-PTFE GDE with mass ratio of $M_{graphite}$:M_{GE}:M_{PTFE} = 8:1:2

For comparison, graphite-PTFE GDE was also prepared using the same method except that no GE was added.

2.3. Electrolysis experiments

The in-situ electrogeneratation of H_2O_2 were carried out with galvanostatic electrolysis method in a three-electrode undivided cell (200 mL) at room temperature, which was controlled by REX DJS-292 potentiostat/galvanostat (Shanghai Cany Precision Instrument Co., Ltd). The prepared

GE/graphite-PTFE GDE (12 cm^2 area) was selected as working electrode, a Pt sheet (6 cm^2 area) and saturated calomel electrode (SCE) as counter and reference electrodes, respectively. The distance between the working electrode and counter electrode was 3 cm. Prior to electrolysis, 200 mL Na_2SO_4 aqueous solution (0.05 mol/L) was added in the undivided cell. The solution was adjusted to the desired pH value (from 1.5 to 8.0) using H_2SO_4 and NaOH and vigorously stirred with a magnetic bar to enhance the mass transport. The solution pH was measured with a Metrohm 654 pH meter (Switzerland). In order to reach high dissolved oxygen concentration for high H_2O_2 production, pure oxygen at 0.02 $m^3\ h^{-1}$ was insufflated into the cell through a porous pipe-diffuser placed right under the cathode. The initial KN-R concentration was 80 mg/L corresponding to 18 mg/L total organic carbon (TOC). The current density changed from 0.5 to 3.0 mA/cm^2 and the concentration of Fe^{2+} changed from 0.1 mmol/L to 1.0 mmol/L. For comparison, using graphite-PTFE GDE as working electrode repeated the above-mentioned experiment in order to evaluate the differences in the electrogeneration of H_2O_2 and dye removal efficience.

2.4. Analytical methods

All samples extracted from the treated solutions were filtered through 25 μm pore size filter paper before analysis. H_2O_2 concentration was analyzed spectrophotometrically (pharmaspec, UV-1700, Japan) by measuring the absorbance at λ = 408 nm (ε = 1010 $M^{-1}\ cm^{-1}$). The cell electric potential was recorded during electrolysis.

The current efficiency (CE) for H_2O_2 formation in the absence of Fe^{2+} is determined as:

$$\mathrm{CE} = \frac{nF[\mathrm{H_2O_2}]V}{Q_\mathrm{t}} \times 100\% \qquad (3)$$

Where n (n = 2) is the number of electrons involved in the electrochemical reaction (1), F is the Faraday constant (96,485 C/mol), [H_2O_2] represents the concentration of H_2O_2 in the reaction solution (mol/L), V is the total volume of electrolytic solution (L), and Q_t is the cumulative charge applied to the system by any given time (C), obtained by integrating the current. TOC analyses were carried out using a Shimadzu 5050 TOC-V_{CPH} analyzer.

After the homogeneous electro-Fenton oxidation, KN-R concentration was also analyzed spectrophotometrically by measuring the absorbance at λ = 580 nm.

3. RESULT AND DISCUSSION

3.1. Electro-generation of H_2O_2

3.1.1. Comparison of electro-generated H_2O_2 on different GDEs

In order to investigate the electro-generation of H_2O_2 on GE/graphite-PTFE and graphite-PTFE GDE, several experiments were performed in the undivided electrolysis system containing 0.05 mol/L Na_2SO_4 (pH 3) at current density of 2.0 mA/cm^2. Fig. 2a shows the change of H_2O_2 concentration with the electrolysis time on different GDEs. With the increase of the electrolysis time, the concentration of

H_2O_2 all increased in two systems. After 180 min electrolysis, the concentration of H_2O_2 produced on GE/graphite-PTFE GDE ($M_{graphite}$:M_{GE}:M_{PTFE} = 8:1:2) was 187.1 mg/L, and it was nearly four times higher than that of graphite-PTFE electrode (47.6 mg/L, $M_{graphite}$:M_{PTFE} = 8:2).

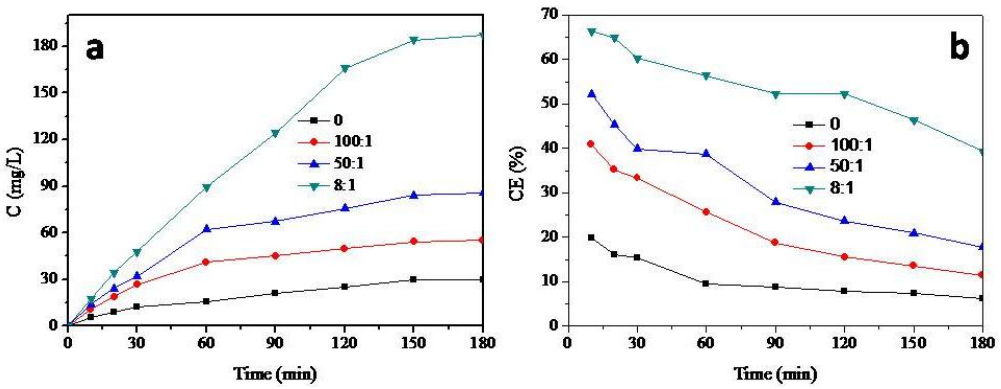

Figure 2. Changes in the electro-generated H_2O_2 concentration **(a)** and current efficience **(b)** with electrolysis time on GE/graphite-PTFE GDE with various mass ratio of $M_{graphite}$:M_{GE}:M_{PTFE}. Conditions: O_2 flow rate of 0.02 m^3/h, 0.05 mol/L Na_2SO_4, pH 3.0, current density of 2.0 mA/cm^2.

The changes in current efficience showed in Fig. 2b exhibts the same trend as that in the accumulated concentration of H_2O_2. It can be attributed to the faster electro transfer accelerated via the introduction of GE in the graphite-PTFE GDE.

3.1.2. Effect of current density on the electro-generation of H_2O_2

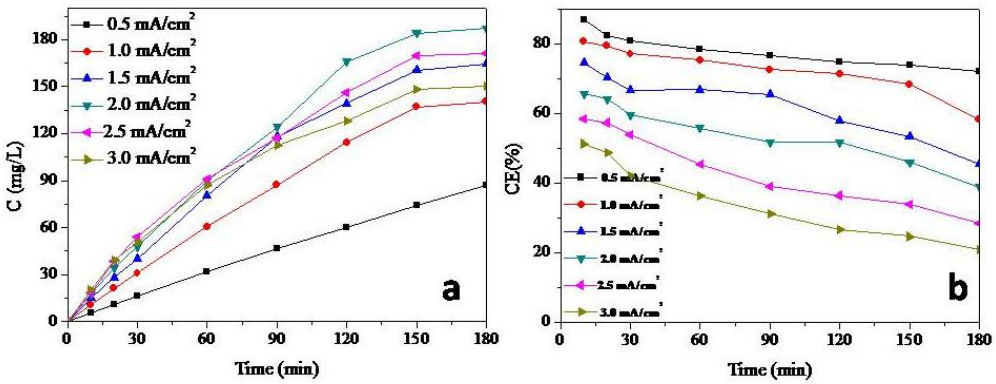

Figure 3. Influence of applied current density on the electro-generated H_2O_2 concentration **(a)** and current efficience **(b)** on GE/graphite-PTFE GDE. Conditions: O_2 flow rate of 0.02 m^3/h, 0.05 mol/L Na_2SO_4, pH 3.0, $M_{graphite}$:M_{GE}:M_{PTFE} = 8:1:2.

Considering that current density had notable influence on the electro-generation of H_2O_2, the electrolysis experiments were also carried out using various current densities ranging from 0.5 to 3.0 mA/cm^2 on GE/graphite-PTFE GDE ($M_{graphite}$:M_{GE}:M_{PTFE} = 8:1:2). As shown in Fig. 3a, the

concentration of H_2O_2 increases as current density increasing from 0.5 to 2.0 mA/cm^2, and then rapidly decreases with the further increase of current density. These results can be explained by the change in cell potential. The average cell potential measured was ca. 1.44, 1.82, 2.47, 3.30, 4.45, 5.37 and 5.89 V during the electrolysis for the applied current density of 0.5, 1.0, 1.5, 2.0, 2.5 and 3.0 mA/cm^2, respectively. It is reported that at the cell potential values higher than 4.45 V, the reduction of O_2 leads to the production of H_2O instead of H_2O_2 through the equation (4) [26], resulting also in the decrease in current efficiency when the applied current density was above 2.0 mA/cm^2 (Fig. 3b).

$$O_2 + 4H^+ + 4e^- \rightarrow 2H_2O \qquad (4)$$

3.1.3. Stability for H_2O_2 electro-generation

Repeated experiments were performed under the conditions of pH of 3.0, current density of 2.0 mA/cm^2 and $M_{graphite}$:M_{GE}:M_{PTFE} = 8:1:2 to examine the reusability of the prepared GE/graphite-PTFE cathode in producing H_2O_2.

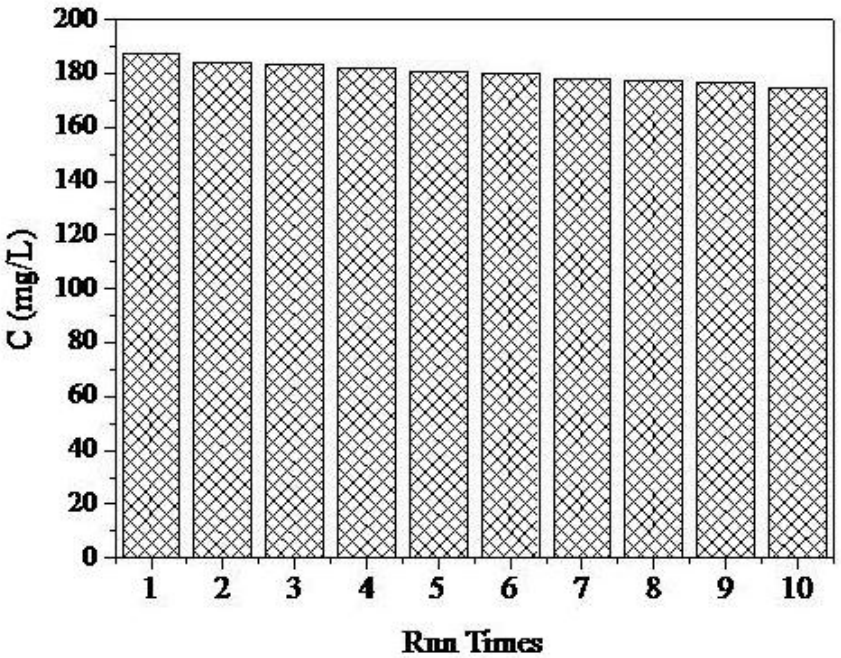

Figure 4. Stability of the GE/graphite-PTFE GDE for the electro-generation of H_2O_2 after 180 min electrolysis. Conditions: O_2 flow rate of 0.02 m^3/h, 0.05 mol/L Na_2SO_4, pH 3.0, current density of 2.0 mA/cm^2, $M_{graphite}$:M_{GE}:M_{PTFE} = 8:1:2.

As shown in Fig. 4, the concentration of electro-generated H_2O_2 declined less 7% from 187.7 to 174.6 mg/L after ten times reuse, indicating the excellent stability of GE/graphite-PTFE GDE for H_2O_2 electro-generation.

3.2. Degradation of KN-R

3.2.1. Effect of solution pH

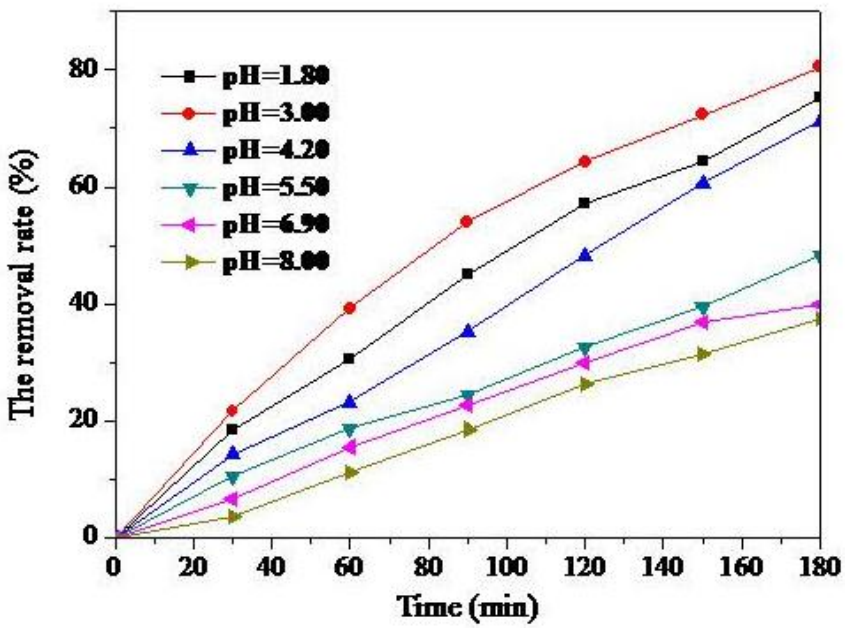

Figure 5. Influence of solution pH on KN-R degradation by homogeneous electro-Fenton process using GE/graphite-PTFE GDE. Conditions: O_2 flow rate of 0.02 m^3/h, 0.05 mol/L Na_2SO_4, current density of 2.0 mA/cm^2, 0.75mmol/L Fe^{2+} and $M_{graphite}$:M_{GE}:M_{PTFE} = 8:1:2.

It was well known that the solution pH was an important parameter for Fenton oxidation process. Fig. 5 presents KN-R decay in various pH solutions (from pH 1.5 to 8.0) containing 0.75 mM Fe^{2+} using GE/graphite-PTFE GDE. As can be seen, electro-Fenton process is effective and the highest oxidation activity is achieved at pH 3.0. About 80% KN-R was removed after 180 min electrolysis, which was entirely consistent with the reported by other authors for the degradation of organic pollutants via the electro-Fenton methods and it is also very close to the optimum pH of 2.8 for Fenton's reaction [27]. At low pH values below 3, the electro-generated H_2O_2 will solvate a proton to form an oxonium ion ($H_3O_2^+$, as shown in equation (5)) which enhanced its stability and lost its activity in Fenton chain reaction.

$$H_2O_2 + H^+ \rightarrow H_3O_2^+ \qquad (5)$$

When the solution pH was above 3.0, the coagulation accompanying with the oxidation simultaneously occurred, involving the formation of hydroxyl-complexes of iron and the polymerization reaction of the subsequent products [28]. The formation of these ferric hydroxide precipitation not only decreases Fe^{2+} regeneration, but also inhibits H_2O_2 formation by partially coating the GE/graphite-PTFE GDE surface, thus reducing electro-Fenton oxidation efficiency. An inspection of the GE/graphite-PTFE GDE conducted in pH > 5.5 disclosed the occurrence of yellow $Fe(OH)_3$ precipitation on its surface.

3.2.2. Effect of Fe^{2+} concentration

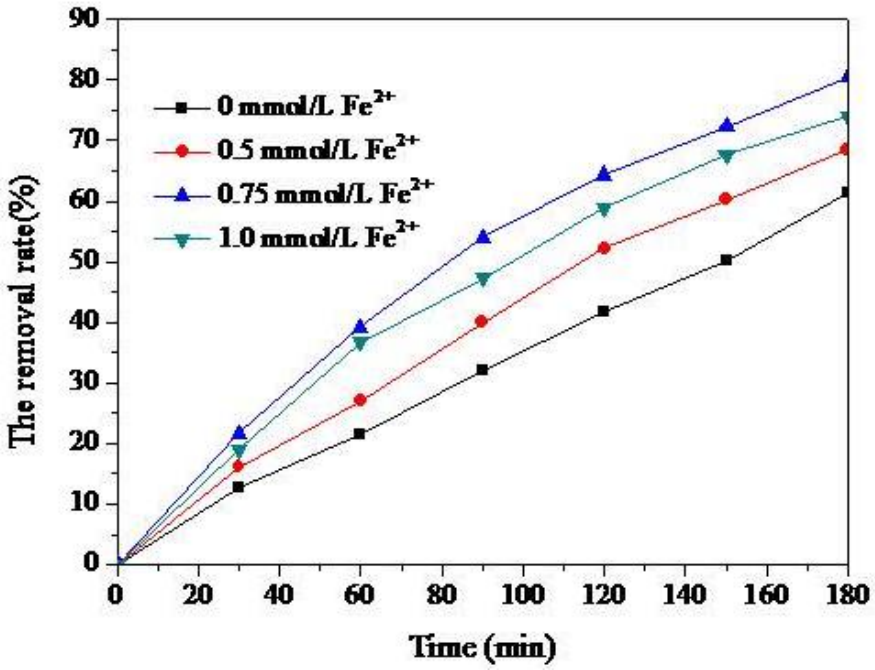

Figure 6. Influence of Fe^{2+}concentration on KN-R degradation by homogeneous electro-Fenton process using GE/graphite-PTFE GDE. Conditions: O_2 flow rate of 0.02 m^3/h, 0.05 mol/L Na_2SO_4, current density of 2.0 mA/cm^2, pH 3.0 and $M_{graphite}$:M_{GE}:M_{PTFE} = 8:1:2.

Organics degradation by electro-Fenton process not only depended on electrogenerated H_2O_2, but also is controlled by the concentration of Fe^{2+} and/or Fe^{3+} as catalyst [6,9]. The effects of initial Fe^{2+} concentrations on KN-R degradation at pH 3.0 are depicted in Fig. 6. Degradation rate undergoes a gradual acceleration when Fe^{2+} concentration increases from 0 to 1.0 mmol/L. It can be seen that the removal rate increased from 60% to 80% when the concentration of Fe^{2+}increased from 0 to 0.75 mmol/L. In the absence of Fe^{2+}, the main oxidant was the electro-generated H_2O_2 which limited oxidation power. The enhanced decay should be attributed to the larger amount production of $HO^{\bullet}$ in the medium with the increasing Fe^{2+}, however, with a further increase of Fe^{2+} concentration to 1.0 mmol/L, KN-R removal rate was declined. It was because that further increase in Fe^{2+} concentration will consume $HO^{\bullet}$ with the following non-oxidizing reaction (equation (6)) [29]:

$$Fe^{2+} + HO^{\cdot} \rightarrow Fe^{3+} + OH^{-} \qquad (6)$$

3.2.3. Change of UV-visible absorption bands

In order to clarify the changes of molecular and structural characteristics of KN-R at different electrolysis time in the electro-Fenton process, UV-visible spectra were measured in the course of oxidation.

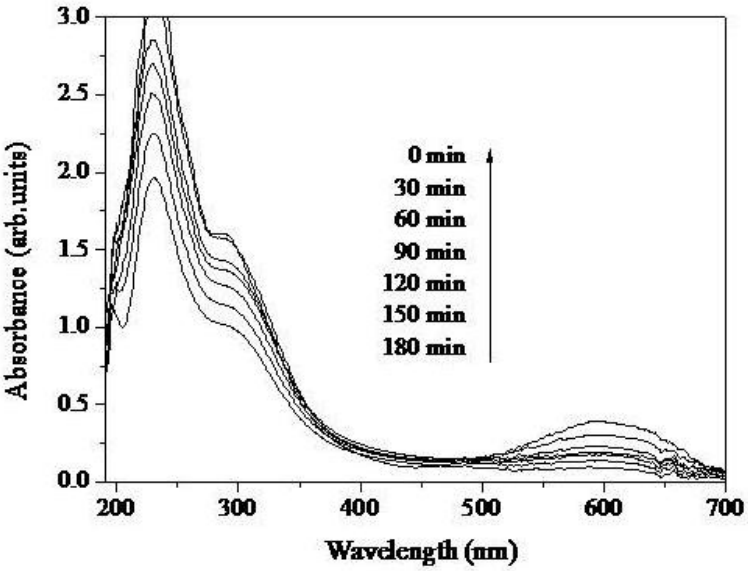

Figure 7. Change in the UV-visible spectra of KN-R with electrolysis time under the optimal electro-Fenton conditions: O_2 flow rate of 0.02 m^3/h, 0.05 mol/L Na_2SO_4, current density of 2.0 mA/cm^2, pH 3.0 0.75 mmol/L Fe^{2+} and $M_{graphite}$:M_{GE}:M_{PTFE} = 8:1:2.

As shown in Fig. 7, KN-R was characterized by one main band in the visible region with the absorption peak at ca. 590 nm, and the other two bandsin the ultraviolet region with absorption peaks at around 310 and 240 nm, respectively. The peak at 590 nm might originate from the formation of hydrogen bond between amino-group and adjacent carbonyl groups in the matrix structure of anthraquinone, which strengthened the conjugate action between lone pair electrons and anthraquinone annulus. The weak absorption band at 310 nm was attributed to the transition of lone pair electrons in carbonyl groups. The characteristic absorption peak at 240 nm was ascribed to the matrix structure of anthraquinone，which embodied the existence of aromatic ring structure. With the electrolysis time extended, the absorption peak at 590 nm rapidly weakens accompanied with the disappearance of solution color, which indicates that the conjugated system of KN-R was destroyed completely. The two bands in the ultraviolet region also decreased due to the damage of aromatic ring structure.

3.2.4. KN-R mineralization

Fig. 8 displays the mineralization of KN-R anthraquinnone dye under the optimality conditions, i.e. pH = 3.0, 0.75 mmol/L of Fe^{2+} concentration, 2.0 mA/cm^2 of current density and $M_{graphite}$:M_{GE}:M_{PTFE} = 8:1:2. As can be seen, maximum 33.3% TOC decay is obtained. This poor mineralization can be related to the formation of intermediate produces such as short carboxylic acid and their complexes with iron ions, which are difficult to be oxidized completely by $HO^{\bullet}$ generated in the medium [7,9,12]. But in the first 90 min a faster degradation is found, which can be accounted for the production of more $HO^{\bullet}$ and that the major produced in this time period, aromatics intermediates can be more easily destructed [9]. The slower Fe^{2+} regeneration rate and the formation of stable Fe^{3+}-carboxylic acid complex, result in lower TOC decay at the second stage. These findings agree well

with the studies of Zhou et al. [5,6] and Brillas et al. [7,9,12] who also found the "platform behavior" during organics mineralization by electro-Fenton and photoelectro-Fenton processes.

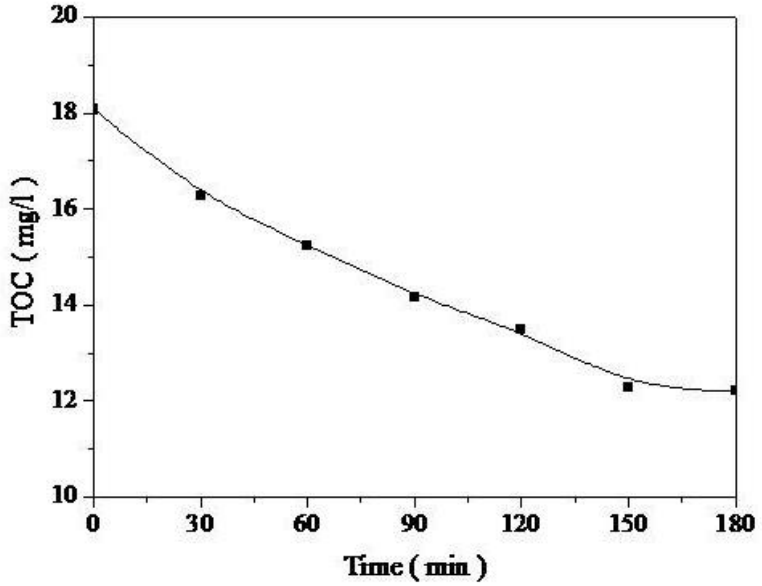

Figure 8. TOC decay of KN-R under the optimal electro-Fenton conditions: O_2 flow rate of 0.02 m^3/h, 0.05 mol/L Na_2SO_4, current density of 2.0 mA/cm^2, pH 3.0 0.75 mmol/L Fe^{2+} and $M_{graphite}$:M_{GE}:M_{PTFE} = 8:1:2.

4. CONCLUSIONS

In this study, GE/graphite-PTFE GDE was prepared and the efficiency of electro-generated H_2O_2 was evaluated by an undivided electro-Fenton system. The amount of electro-generated H_2O_2 using GE/graphite-PTFE GDE ($M_{graphite}$:M_{GE}:M_{PTFE} = 8:1:2) was nearly three times higher than that of graphite-PTFE GDE ($M_{graphite}$:M_{PTFE} = 8:2) due to the accelerated electron transfer rate resulting from GE. The highest H_2O_2 concentration was obtained at pH 3.0 and the current density of 2.0 mA/cm^2. KN-R could be degraded quickly and efficiently by the proposed electro-Fenton process using GE/graphite-PTFE GDE. Under the pH 3.0 and 0.75 mmol/L Fe^{2+} concentration, ca. 80% KN-R with the initial concentration of 80 mg/L could be degraded and 33.3% mineralization rate was achieved after 180 min electrolysis.

ACKNOWLEDGMENTS
The authors would acknowledge the financial support from the National Natural Science Foundation of China (No.20977012, No.21177017 and No.21177019), the Post-Doctoral Science Foundation of China (No. 2011M500560) and the Fundamental Research Funds for the Central Universities (No. DUT13LK50).

References

1. M.A. Brown and S.C. De Vito, *Crit. Rev. Environ. Sci. Technol.*, 23 (1993) 249
2. V. Meshko, L. Markovska, M. Mincheva, and A.E. Rodrigues, *Water Res.*, 35 (2001) 3357

3. C. Galindo, P. Jacques, and A. Kalt, *Chemosphere*, 45 (2001) 997
4. M.C. Venceslau, S. Tom, and J.J. Simon, *Environ. Technol.*, 15 (1994) 917
5. M.H. Zhou, Q.H. Yu, and L.C. Lei, *Dyes Pigments*, 77 (2008) 129
6. M.H. Zhou, Q.H. Yu, L.C. Lei, and G. Barton, *Sep. Purif. Technol.*, 57 (2007) 380
7. E. Isarain-Chavez, R.M. Rodriguez, J.A. Garrido, C. Arias, F. Centellas, P.L. Cabot, and E. Brillas, *Electrochim. Acta*, 56 (2010) 215
8. Z.H. Ai, T. Mei, J. Liu, L.Z. Zhang, K.J. Deng, and J.R. Qiu, *J. Phys. Chem. C*, 112 (2008) 11929
9. C. Flox, S. Ammar, C. Arias, E. Brillas, A.V. Vargas-Zavala, and R. Abdelhedi, *Appl. Catal. B: Environ.*, 67 (2006) 93
10. Ch. Comninellis, Electrochim.Acta 39 (1994) 1857
11. E. Brillas, R. Sauleda, and J. Casado, *J. Electrochem. Soc.*, 145 (1998) 759
12. S. Randazzo, O. Scialdone, and E. Brillas, *J. Hazard. Mater.*, 193 (2011) 1555
13. A. Wang, J. Qu, H. Liu, and J. Ru, *Appl. Catal. B: Environ.*, 84 (2008) 393
14. Y.R. Wang and W. Chu, *Water Res.*, 45 (2011) 3883
15. J.S. Do and C.P. Chen, *J. Appl. Electrochem.*, 24 (1994) 936
16. S. Murugesan, K. Myers, and V.R. Subramanian, *Appl.Catal. B: Environ.*,103 (2011) 266
17. A. Dhaouadi, L. Monser, and N. Adhoum, *Electrochim. Acta*, 54 (2009) 4473
18. N. Daneshvar, S. Aber, V. Vatanpour, and M.H. Rasoulifard, *J. Electroanal. Chem.*, 615 (2008) 165
19. S. Hammami, N. Oturan, N. Bellakhal, M. Dachraoui, and M.A. Oturan, *J. Electroanal. Chem.*, 610 (2007) 75
20. A.A. Gallegos and D. Pletcher, *Electrochim. Acta*, 44 (1999) 2483
21. C.P. Leon and D. Pletcher, *J. Appl. Electrochem.*, 25 (1995) 307
22. A.K. Geim, *Science* 24 (2009) 1530
23. A.K. Geim, K.S.Novoselov, S. V.Morozov, D. Jiang, Y. Zhang, and S. V. Dubonos, *Science* 306 (2004) 666
24. W.S. Hummers and R.E. Offeman, *J. Am. Chem. Soc.*, 80(1958) 1339
25. N.I. Kovtyukhova, P.J. Ollivier, B.R. Martin, T.E. Mallouk, S.A. Chizhik, and E.V. Buzaneva, *Chem. Mater.*, 11 (1999) 771
26. A. Özcan, Y. Sahin, and M.A. Oturan, *Chemosphere* 73 (2008) 737
27. B.G. Kwon, D.S. Lee, and N. Kang, *Water Res.*, 33 (1999) 2110
28. L. Szpyrkowicz, C. Juzzolino, and S.N. Kaul, *Water Res.*, 35 (2001) 2129
29. M. Panizza and G. Cerisola, *Water Res.*, 35(2001) 3987